Novel calibration method for optical coherence tomography instruments using multiple spectrometers

Gianni Nteroli,[a,*]Lucy Abbott,[a] Rasmus D. Engelsholm,[b] Patrick Bowen Montague,[b] Adrian Podoleanu,[a] and Adrian Bradu[a]

[a]Applied Optics Group, School of Physics and Astronomy, University of Kent, Canterbury, UK
[2]NKT Photonics A/S, Blokken 84, DK-3460, Birkerød, Denmark

ABSTRACT

In this report, a novel calibration method is introduced, which can be used in camera-based optical coherence tomography (OCT) instruments employing several spectrometers. To ensure that all spectrometers are calibrated, i.e. they sense the same spectral range and the distribution of the optical frequencies across the pixels of the cameras is the same, a hybrid method was used involving (i) a hardware procedure for an initial estimation of the edges of the spectra and (ii) a numerical Monte-Carlo based technique. The utility of such a procedure is demonstrated in an OCT system using a balance-detection (BD) scheme. The OCT system employs a single transmission diffraction grating and is driven by a supercontinuum source operating in the visible spectral range. Spectral alignment is paramount in producing high-sensitivity images free of artefacts. To ensure correct calibration, and speed up the calibration procedure, the master-slave (MS) technique of generating axial reflectivity profiles is employed. Preliminary results show an improvement of the signal of ~ 3dB and a mitigation of the background noise of over 5 dB.

Keywords: balanced detection, axial resolution, visible optical coherence tomography, spectral alignment

1. INTRODUCTION

Conventional OCT allows non-invasive, *in-vivo*, imaging of the retina with axial resolutions of several micrometres. Although both, swept-source (SS) and camera-based (CB) implementations of the OCT enable high imaging speeds, with excellent sensitivity. Currently, only CB instruments have been demonstrated in the visible (VIS) spectral range where axial resolutions several times better than in the near-infrared (NIR) is achievable. In contrast to NIR-OCT instruments using either, swept-lasers or super luminescent diodes (SLDs), VIS-OCT instruments use supercontinuum (SC) lasers.

Unfortunately, the emission of the SC lasers presents optical power oscillations that lead to relative intensity noise. These power instabilities are spectrally dependent, therefore the noise fluctuates from pixel to pixel across the line-scan camera and as a result, the measured channelled spectra are corrupted, their contrast is lowered, and the final produced images exhibit increased background noise obscuring anatomical structures. A solution to mitigate this noise is to increase the acquisition time of the camera. By doing so, the exposure time of the retina to light is increased, the acquisition time of the data needed to reconstruct an image also increases, and the images hence generated are prone to motion artefacts. As a result, techniques such as image registration and averaging conventionally used to enhance the contrast or generate angiographic views are not efficient. To our knowledge, currently, there is no effective solution to generate high-speed A-scans with high-resolution, and high sensitivity in VIS-OCT. A solution is the use of a balanced detection (BD) configuration, provided that the spectrometers are correctly aligned to cancel the coherent part of the excess photon noise [1]. In most of the existent reports, limited improvements of 3-6 dB in signal intensity with some limited noise reduction were reported, mainly due to the imperfect calibration of the spectrometers [2,3]. Here a novel technique to calibrate two (or more) spectrometers is demonstrated, based on using Monte-Carlo simulations and the Master-Slave technique [4], technique which has the potential to overcome some limitations of the current approaches.

2. EXPERIMENTAL SET-UP AND METHOD

A schematic diagram of the BD OCT interferometer is depicted in Fig. 1. Light from a prototype supercontinuum source (NKT Photonics), after being band-pass filtered is split towards the sample and reference arm by a directional coupler (DC_1, 10/90, respectively sample/reference). In the sample arm, light is conveyed towards the object to be imaged via a pair of galvo-scanners (GXY) and two achromat lenses (L_1 and L_2). Light back-scattered by the sample and light from the

reference arm are superposed in the 50/50 directional coupler DC_2. Light from the two outputs of DC_2 is finally incident on a transmission diffraction grating (TG). The incidence angles between the two collimated beams emerging from DC_2 and the normal to TG were adjusted to match the incidence angle specified by the manufacturer of the grating. Thus, a single TG is used to devise both spectrometers. The line-scan cameras employed here (Basler spL4096-140km), were operated at 140 kHz.

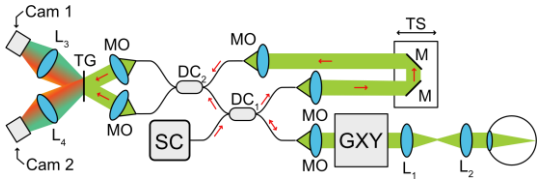

Figure 1. Schematic diagram of the BD instrument. MO: achromatic microscope objectives, $L_{1\text{-}4}$: achromatic lenses; $DC_{1,2}$: directional couplers; M: flat mirrors; TG: transmission grating; TS: translation stage; SC: supercontinuum laser; GXY: pair of galvo-scanners.

Let ***a*** and ***b*** be the pixels on a camera detecting the smallest and the largest value of the frequencies between which the spectra of the source spread respectively. The first spectrometer senses the spectrum between pixels a_1 and b_1 whereas the second one from a_2 to b_2. The non-linear distribution of optical frequencies over the linear array of the camera employed by the two spectrometers are g_1 and g_2 respectively, whereas the dispersion left unbalanced in the interferometers is characterized by the functions h_1 and h_2 respectively. The two spectrometers are perfectly calibrated when the values of a_1, a_2, b_1 and b_2 are correctly determined and when g and h are known. Determining the values of the a and b with high accuracy is not trivial. One simple way to find their values could be by using a bandpass filter with very steep edges, transmitting light over a spectral range matching that of the optical source. If for example, the spectral bandwidth of the optical source is 100 nm, and we aim to cover 4,000 pixels on the cameras, it means that each pixel covers 0.025 nm, which is at least X10 smaller than the edge steepness of the available ultra-steep filters. Instead of using a single bandpass filter, one can use two narrow bandpass filters, with central transmissions towards the limits of the spectra sensed by the cameras. In our experiment, we used two bandpass filters (bandwidth 25 nm), one centered at 550 nm and the other one at 650 nm. They were sequentially placed in the reference arm of the interferometer and spectra were collected with the sample arm blocked. This procedure allowed us to initially compute the frequencies associated to pixels a_1, a_2, b_1 and b_2 with an error determined by the edge steepness of the filters employed. The conventional procedure to calibrate the two spectrometers would involve computing g_1, g_2, h_1, h_2, resample and correct for dispersion of the experimental spectra.

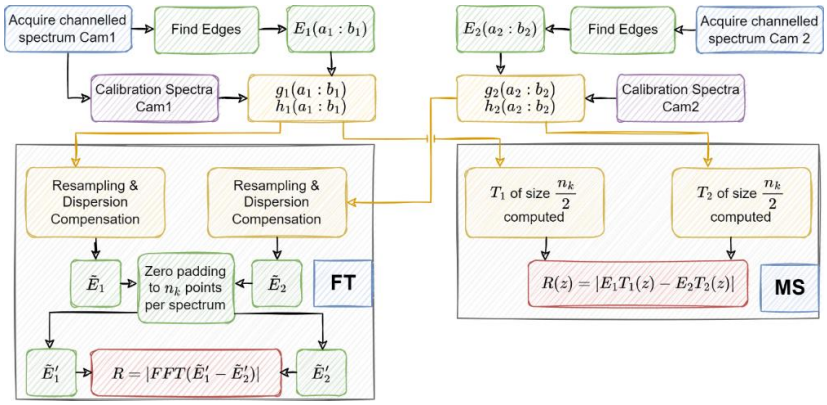

Figure 2. Flowchart showing the steps needed to compute the A-scans using the FT and the MS procedures. $\tilde{E}_{1,2}$ are channelled spectra of equal number of samples obtained by interpolation. $T_{1,2}$ are theoretical infered spectra.

An A-scan is generated by calculating the Fourier transform (FT) of the difference between these resampled spectra. This procedure is illustrated in the flowchart shown in Fig. 2 (FT branch, on the left). Its drawback is the long processing time due to the resampling required. We achieved the alignment of the spectra, by slightly adjusting the values of a_1, a_2, b_1 and b_2 randomly, therefore repeating the calculation for the g and h functions, and resampling and correcting for unbalanced dispersion until a satisfactory result is obtained. The computation of the g and h functions is quite simple and does not involve time-expensive numerical computations, however, the resampling of the spectra, being based on a cubic spline procedure is computationally expensive. For this reason, instead of the FT procedure, we opted for the Master-Slave approach, which does not require data resampling. Instead, only theoretically inferred channelled spectra must be computed for each g and h set of values, which involves very simple mathematical computations [4]. This approach is illustrated in Fig. 2 (MS branch, on the right).

3. RESULTS AND CONCLUSION

Spectra were collected in the following two scenarios: (i) Channeled spectra covering all pixels of the camera were collected for different axial positions, by adjusting the optical path difference between the arm lengths of the interferometer. For these measurements, as a sample, a flat mirror was employed. These spectra were used at the master stage of the MS procedure. (ii) For an initial estimation of the a_1, a_2, b_1 and b_2, the sample arm was blocked, whereas, in the path of the light in the reference arm two bandpass filters were introduced sequentially and spectra were collected.

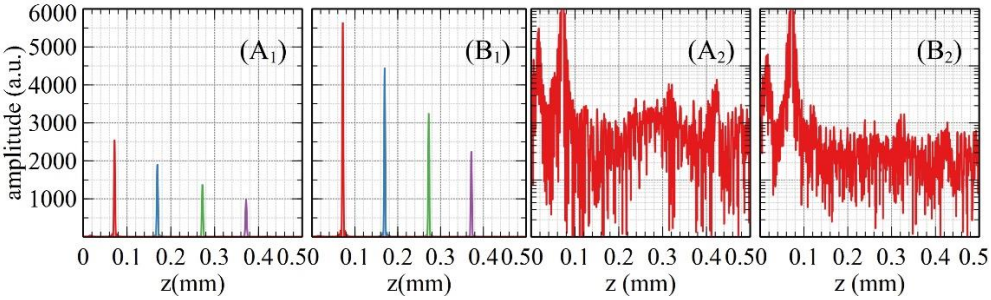

Figure 3. Axial sensitivity roll-off produced using one spectrometer (A1) and the BD configuraion (B1). (A2): single A-scan produced using one spectrometer; (B2): single A-scan produced using a BD configuration (log scale).

Random values for $\tilde{a}_i \in (a_{1,2} - \delta a, a_i + \delta a)$ and $\tilde{b}_i \in (b_{1,2} - \delta b, b_i + \delta b)$, where δa and δb determine the range the random numbers were generated (i =1,2). For each set of values of $\tilde{a}_i, \tilde{b}_i$, g and h were calculated, theoretical masks were recomputed and MS-based A-scans were produced. The simulation was stopped after 10,000 iterations. The best set of numbers $\tilde{a}_i, \tilde{b}_i$ for which the highest amplitude of the A-scan peak or the minimum value of the background noise was obtained, and can be used for imaging purposes. However, we have noticed that a better strategy in terms of improvement of both the signal and mitigating noise can be obtained if the set of values $\tilde{a}_i, \tilde{b}_i$ for which $\sum_j^N |R_j^{max}|$ has its highest value is selected. $|R_j^{max}|$ is the maximum value of the A-scan peak measured for an axial position z_j (N is the number of channeled spectra used). The plots shown in Fig. 3 were produced by using this strategy. In Fig. 3(A1), a typical sensitivity drop-off obtained using one spectrometer is presented, whereas to produce Fig. 3(B1), the BD was employed. It is quite obvious, and expected, that the signal in the BD configuration to be enhanced, by >3dB in our case, for all axial positions. To better visualize a possible reduction of the background noise, in Figs. 3(A2) and 3(B2), we show in log scale, only one of the A-scans. It is noticeable that in the BD configuration, the noise drops. By calculating the RMS value of the signals over the range 0.1 – 0.5 mm, we found that the noise floor is lower by typically 5.5 dB when the balanced configuration is employed. Additional details on the hardware employed, the theoretical approach behind the simulation approach, and a demonstration of the improvements due to the BD in images, will be presented at the conference.

Acknowledgements

AP and AB acknowledge the support of BBSRC project, BB/S016643/1. AP acknowledge the EU's Horizon 2020 programme (Marie-Curie grant 860807), the NIHR Biomedical Research Centre, UCL Institute of Ophthalmology, and Royal Society Wolfson research merit award. AB also acknowledges the support of the Royal Society, project PARSOCT, RGS/R1/221324 and the support of the Academy of Medical Sciences/the Welcome Trust/the Government Department of Business, Energy and Industrial Strategy/the British Heart Foundation/Diabetes UK Spring-board Award SBF007\100162. LA and GN acknowledge the support of the University of Kent.

[1] Jensen, M., Gonzalo, I., Engelsholm, R., Maria, M., Israelsen, N., Podoleanu, A., and Bang, O., "Noise of supercontinuum sources in spectral domain optical coherence tomography," J. Opt. Soc. Am. B 36, A154-160 (2019).

[2] Bradu, A., and Podoleanu, A., "Fourier domain optical coherence tomography system with balance detection," Opt. Express 20, 17522-17538 (2012).

[3] Rubinoff, I., Miller, D., Kuranov, R., Wang, Y., Fang, R., Volpe, N., and Zhang, H., "Balanced-detection visible-light optical coherence tomography," Biorxiv, (2021).

[4] Bradu, A., Israelsen, N., Maria, M., Marques, M., Rivet, S., Feuchter, T., Bang, O., and Podoleanu, A., "Recovering distance information in spectral domain interferometry," Scientific Reports 8, 15445 (2018).